Vrije Universiteit Amsterdam

Universiteit van Amsterdam

Master Thesis

KM3NeT Neutrino (Deep Learning|Neural Networks) Detection

Author: Arumoy Shome (2636393)

1st supervisor:	Dr. Adam Belloum	
2nd supervisor:	Ben van Werkhoven	(Netherlands eScience Center)
2nd reader:	Dr. FINDME	

A thesis submitted in fulfillment of the requirements for the joint UvA-VU Master of Science degree in Computer Science

October 7, 2020

Abstract

Here goes the abstract of this thesis.

Contents

List of Figures

LIST OF FIGURES

List of Tables

LIST OF TABLES

1

Introduction

Perhaps the most elusive subatomic particle known to science is the Neutrino. With no electrical charge (thus aptly named) and mass smaller than any other elementary particles, neutrinos simply pass through other matter making them virtually undetectable. However, neutrinos are sought after by researchers especially the ones working in the fields of Astrophysics and Astronomy since they may help us gain insights into astronomical events such as the birth of a neutrino star or a supernova.

When neutrinos experience a change in the density of the matter they are passing through(such as going from air into water), they experience a change in velocity thus emitting an electron and a photon. This phenomenon is known as Cherenkov Radiation (1) and is an indirect method which can be used to detect neutrinos. In fact, this remains the premise for some of the worlds largest neutrino observatories built to date such as the Sudbury Neutrino Observatory (Ontario, Canada), The Super-Kamiokande (Gifu Prefecture, Japan) and The IceCube Neutrino Observatory (Antarctica).

The KM3NeT or the Cubic Kilometer Neutrino Telescope is the next generation neutrino telescope, currently being constructed at the bottom of the Mediterranean Sea. The goal of this research infrastructure is two fold. First, is to study high energy neutrinos originating from celestial events in the galaxy. And second, to study the properties of the neutrino particles produced in the Earth's atmosphere (2). The first goal will be realized with the KM3NeT/ARCA (Astroparticle Research with Cosmics in the Abyss) telescope and the second with KM3NeT/ORCA (Oscillation Research with Cosmics in the Abyss) (2). In this paper, we talk exclusively about KM3NeT/ARCA.

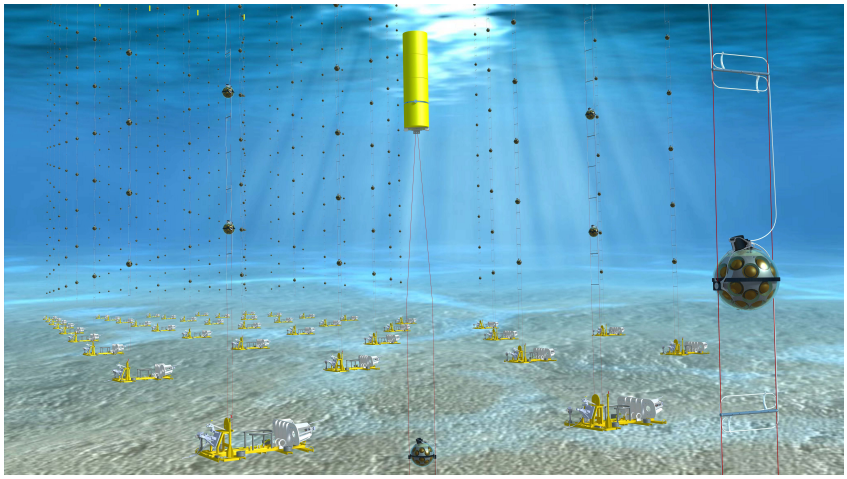

Figure 1.1: Artist's impression of the ARCA detector *source: https://www.km3net.org*

Figure 1.2: An optical detector (DOM) *source: https://www.km3net.org*

1.1 Situation of Concern

The ARCA telescope comprises of two "blocks" with a total volume of $1km^3$. Each block consists of 115 spherical detector units (DOMs) and each DOM consists of 31 Photo Multiplier Tubes (PMTs) in various spacial arrangement. Figure 1.1 shows an artist's impression of ARCA, figure 1.2 depicts a DOM along with the PMTs inside it. The PMTs are highly sensitive to light (photons), and thus are used to detect the Cherenkov Radiation of neutrino particles. The analog signal for all hits above a certain threshold are digitized. This datapoint consists of a timestamp and the spatial orientation of the DOM (ie. x,y,z coordinates). The digital signals from all PMTs are arranged in 100ms "timeslices" and sent to the on-shore facility for further processing (3).

Unfortunately, there are several sources of noise (in this case, the noise is other light sources), bioluminescense and decay of Potassium 40 (^{40}K) and atmospheric Muons being the primary sources (4). Due to the high level of noise, data is generated at an extremely high rate of 25GB/sec (2) and must be filtered and selectively stored for further analysis. The state of the art for this task are known as "Event Trigger" algorithms (2, 3) which can filter timeslices containing just noise thus only allowing important timeslices containing neutrino hits to pass through. The existing event trigger algorithms namely *L1* and *L2* although able to conduct the filtration in near real, lack the ability to do so with high accuracy thus often failing to save important timeslices (5). Efforts have already been made to improve the existing event trigger algorithms. Karas et al. proposed and implemented a GPU powered pipeline which utilizes correlation and graph community detection to

identify time slices that may contain neutrino hits whilst (4) suggests an alternate using convolutional neural networks.

1.2 User Requirements

The primary users of the ARCA are researchers who want to study high energy particles from outer space. The stakeholders are all member institutes involved in the project and by extension all scientists from these institutes who will be working with the data collected.

The requirements of the primary users (and stakeholders) with respect to the data acquisition pipeline are as follows.

UR1. **The accuracy of filtration must be extremely high.**

Time slices which are deemed important by event trigger algorithms are stored for further analysis and research. Failure to store timeslices containing information from neutrino events can lead to loss of important data and thus a poor quality of research. Since majority of the data generated is noise, the pipeline must be able to prevent storage of unnecessary timeslices containing only noise in the on-shore facility.

UR2. **Filtration should occur in real time.**

The state of the art event trigger algorithms are able to process data in real time. The proposed alternative ideally should maintain or improve upon it's predecessor's performance else provide a good trade off with data quality.

1.3 Research Question

This report intends to improve upon *The Karas Pipeline*, a GPU pipeline proposed by Karas et al. to combat the limitations of the L1 and L2 event trigger algorithms. Specifically this project sought to answer the following research questions.

RQ1. **Can the existing GPU pipeline be improved using neural networks (NNs)?**

Improvement may be achieved by reducing the processing time of the pipeline or improving the accuracy of identifying important timeslices. This project focuses on achieving improvement via accuracy and the task of validating the runtime performance of the methods proposed in this paper is left to a separate project.

In order to answer **RQ1**, the following sub questions are formulated.

RQ2. Can the *Hit Correlation Step* be replaced with a Multi Layer Perceptron?

The first step of The Karas Pipeline is the Hit Correlation Step, a novel trigger criterion which given a pair of points, can quantify the level of correlation amongst the points with an accuracy of 80%. The first phase of this project focuses on achieving better accuracy to identify "causally related" points using a Multi Layer Perceptron (MLP).

RQ3. Can the *Graph Community Detection Step* be replaced with a Graph Convolusional Neural Network?

The output of the Hit Correlation Step is used to create a graph structure where hits (of neutrino and noise) are represented as nodes and causally related nodes are connected with an undirected edge carrying the probability of correlation as its weight. The Constant Pots clustering algorithm, which operates on the principles of Graph Community Detection, is used to separate the graph into communities of neutrino and noise hits. The second phase of this project focuses on achieving a better accuracy for clustering neutrino and noise hits into separate communities in a given timeslice using Graph Convolusional Neural Networks (GCNs).

The following chapters of this report present the research efforts carried out to improve The Karas Pipeline using Artificial Neural Networks. In Chapter 3 the steps taken to prepare the dataset used in this project is presented followed by its statistical analysis and visual exploration in Chapter 4. Since this research initiative is a direct offshoot of the work previously conducted by Karas et al., an overview of The Karas Pipeline is presented in Chapter 2. Chapters 5 and 6 present detailed analysis of the neural networks created to replace segments of The Karas Pipeline. Drawing from the results of the replacement models, practical recommendations and directions for further research are laid out in Chapter 7. This report is intended for the primary users of ARCA with the hope to aid in the development of the successor to the state of the art event trigger algorithms. The report may also be used by deep learning practitioners working in the field of neutrino detection. This report assumes the reader posses a background in Computer Science or Artificial Intelligence and thus is familiar with concepts such as statistics, linear algebra and optimization. The reader is expected to have basic understanding of the guiding principals of Deep Learning such as Feed-Forward Neural Networks, backpropagation, binary classification and model evaluation metrics.

2

The Karas Pipeline

This chapter presents the GPU pipeline proposed by (5) (henceforth referred to as the *Karas Pipeline* in more detail since the work presented in this report is directly based off of this seminal work. The chapter concludes by presenting the limitations of the Karas Pipeline and derives motivations for a better alternative as presented in the following chapters (see chapters **??** and **??**).

Karas et al. presents a data processing pipeline to filter timeslices containing hits from neutrino events from those containing only noise. The pipeline is able to achieve this filtration by processing the data in 3 steps, illustrated in Figure 2.1 and described in more detail below. Figure 2.2 provides a visual representation of the various shapes and arrangements of the data as it passes through the pipeline.

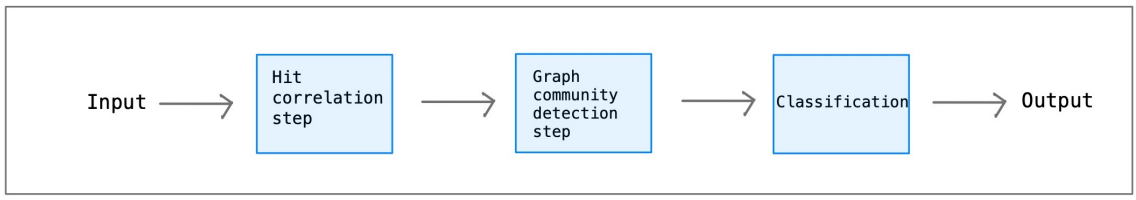

Figure 2.1: Overview of Karas Pipeline

The first step of The Karas pipeline is the Hit Correlation step. In this step, pairs of hits (from events and noise) are considered and the correlation along two axes namely space and time are considered. Karas et al. proposes *The Pattern Matrix Criterion (PMC)*. The PMC operates by creating a correlation criterion based on the probability that a given space and time difference occurs between two event hits. From domain knowledge, the evaluation is limited to 100m and 300ns for space and time differences respectively. The algorithm is evaluated with a dataset containing 130 event hits and 5000 noise hits and

scores in the range of 0.3 - 0.375 is reported for the recall, precision and F1 metrics and an accuracy of 80% is achieved.

The second step of the Karas pipeline is the Graph Community Detection step. The Constant Potts Model (CPM) is used to group event and noise hits (represented as nodes of a graph) into separate communities (or clusters) based on the density of connections and the size of the communities. The output of the PMC is utilized to connect causally related nodes with an undirected edge and the probability of correlation is assigned as the weight of the edge. The model is tested using a dataset consisting of 130 event hits and 5000 noise hits. The model is able to perform exceptionally well and groups most event hits into a single community and the noise in another. No performance metrics are reported however.

The third and final step of the pipeline is the Classification step. The two parameters namely the Probability Threshold (PT) of the PMC and the γ of the GCD step are experimented with to determine the optimal thresholds. All hits above the specified thresholds are classified as event hits the rest are classified as noise.

2.0.1 Limitations of the Karas Pipeline

The Karas Pipeline is able to identify timeslices with neutrino event hits more accurately compared to its predecessors such as the L1 and the L2 filtration. However, the pipeline still has certain limitations which hinders its performance, thus motivating a need for a better alternative.

To begin, the space and time difference based on which the PMC determines if two hits are causally related to one another, is static. This results in event hits which do not meet these thresholds to be incorrectly given a low probability of correlation to its sibling (related) hits.

The performance of the GCD step directly depends on the output of the PMC since the edges between causally related nodes and the weight it carries is determined from the PMC. Thus, any limitations of the PMC cascade down into the GCD and by extension, also into the classification step.

The CPM creates communities by observing the density of connections and the size of the communities. These thresholds are once again static which results in small communities being overlooked.

Finally, the classification step also operates on static values of the PT and γ and thus is unable to identify communities of size smaller than 20 hits.

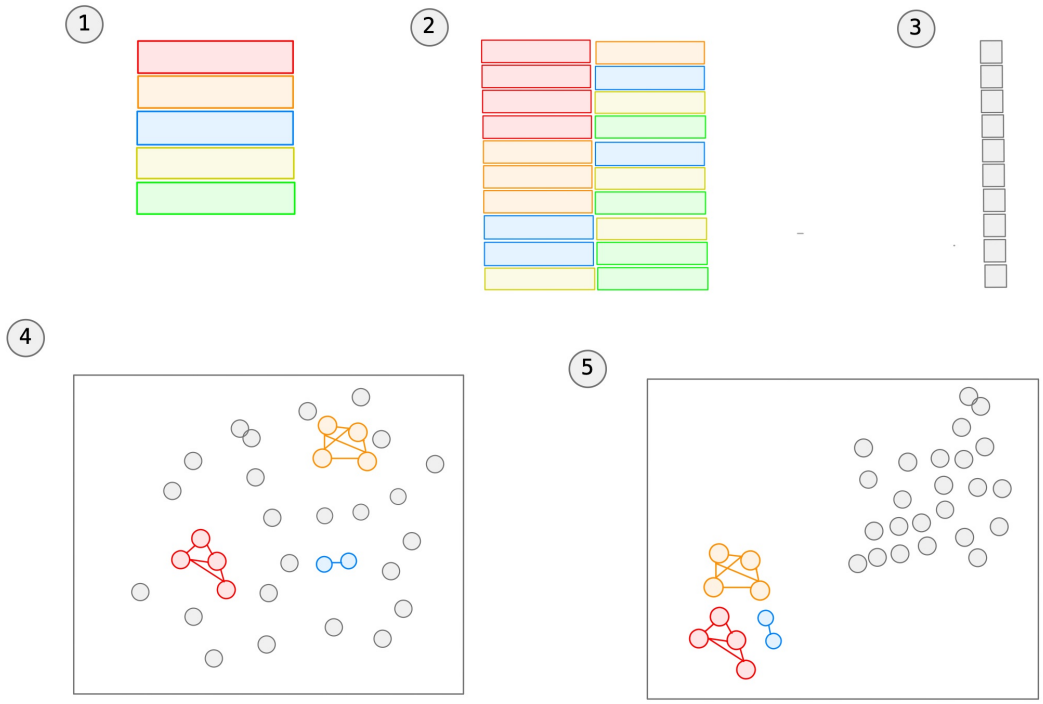

Figure 2.2: **(1)**. The main dataset of the project, each row representing a hit consisting of the (x, y, z, t)*vector*. Here an example set containing 5 hits is shown. **(2)**. The input to the Correlation Step is all unique pairs of hits. **(3)**. The output of the Correlation Step is a vector containing the probability that the pairs of hits are related to each other. **(4)**. (1) and (3) are used to construct a graph representation of the dataset where event (red, orange and blue) and noise (grey) hits are represented as nodes and related nodes are connected by an undirected edge carrying as weight the probability of being related. **(5)**. The graph from (4) acts as the input to the Graph Community Detection step, the output of which is another graph where event and noise nodes are grouped together and thus are linearly separable from each other.

3

Data Preparation

At the time of undertaking this project, the KM3NeT Neutrino Telescope was still under construction, thus simulated data provided by Nikhef was used for the project. The data itself was split onto two parts namely *events* and *noise*, both of which came from different sources and in different formats.

3.1 Preparation of *events* dataset

The *events* dataset was provided as a *HDF5* (Hierarchical Data Format) with a size of 42MB consisting of the `/data/mc_hits` and `/data/mc_info` tables. For the purposes of this project, the two tables were combined such that each row in the *mc_hits* table contains it's corresponding 'event_id' from the *mc_info* table. A `label` column was added containing a value of '1' and the resulting table (henceforth referred to as the *events* dataset) was saved as a CSV file for future use.

3.2 Preparation of *noise* dataset

The *noise* data was generated using a Python library written and maintained by Nikhef, `k40gen`. `k40gen.Generators(21341, 1245, [7000., 700., 70., 0.])` was used to create an instance of a generator where the first two arguments are random seeds followed by a list of rates at which single, double, triple and quadruple hits should be generated. The generator instance is then passed into `k40gen.generate_40()` method which returns a (4, n) array containing (time (t), dom_id, pmt_id, time over threshold (tot)). The position coordinates (ie. `x`, `y`, `z` coordinates) for each datapoint was provided in a *positions.detx* file which was parsed using the Numpy Python package (6) and added to the *noise* array.

The Python library Pandas (7) was used to convert the array into a (n, 4) dataframe. A `label` column was added containing a value of '0' and the dataframe was saved as a 3.9GB CSV file.

3.3 Preparation of *main* dataset

To create the *main* dataset for the project, the *events* and *noise* datasets were combined. Both datasets were read into memory as Pandas dataframes and their columns were renamed consistently. The two dataframes were concatenated and sorted based on the `time` column. Rows with a negative `time` value were dropped along with columns which are not relevant to this project. The `time` column was discretized into 15000ns bins and the resulting values were added to the `timeslice` column. The resulting dataframe was saved as a 1.9GB CSV file.

4

Data Exploration

The *main* dataset (generated as per the steps outlined in Chapter 3) was explored using statistical analysis and visualizations to observe any patterns and "local trends" that may be present. The following chapter presents the analysis that were done and the observations made.

Note that a random sample of only 10% of the data was taken for the following visualizations. This is because it is difficult to draw reasonable conclusions from the plots due to the high number of data points when the entire dataset is used.

4.1 Descriptive Statistics

Table 4.2 presents the descriptive statistics of the *main* dataset. The dataset consists of 7 columns and roughly 4.5 million rows, Table 4.1 provides more information on the columns on the dataset. The dataset does not contain any `nan` or `null` values except for the `event_id` column where rows containing noise hits are not associated with any event.

Next, the correlations amongst features is checked, the "Pearson" correlation is used. Figure 4.2 represents the correlation matrix of all features. No significant correlations are observed between `x`, `y`, `z` and `t` which indicates that ML models may not be able to learn anything from the dataset without the aid of feature engineering.

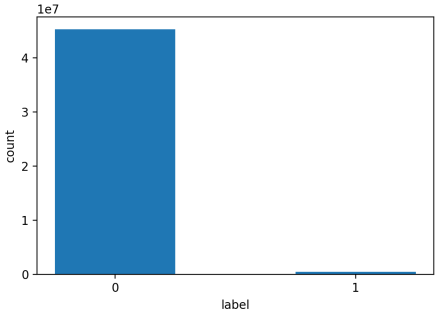

Figure 4.1: Distribution of `label` column

Table 4.1: Description of columns

Column	Data type	Unit	Description
x, y, z	float	meters (m)	The position within the detector where the hit was detected, they represent the x,y,z coordinates of the hit respectively.
t	float	nano seconds (ns)	The time at which the hit was detected.
label	int	NA	The type of hit, '0' represents noise and '1' represents a neutrino hit
event_id	int	NA	The id of the event to which the hit is related to. The id itself does not have any meaning, it is simply used to identify hits that originated from the same event.
timeslice	int	NA	The id of the timeslice to which the hit belongs. The id itself does not have any meaning, it is simply used to group hits into discrete bins.

The distribution of the `label` column is presented in Figure 4.1. A severe class imbalance is noted between events and noise hits. To be precise, the dataset contains 489906 instances of events compared to over 4.5 million instances of noise. An effective strategy to handle the class imbalance will need to be devised during training of models to prevent the model from overfitting.

4.2 Verification of Bias

The *events* dataset is synthetically generated using simulations. As such, it is likely that the event hits in each timeslice may occur at a specific time such as at the beginning, middle or end of the timeslice. Having such a pattern in the dataset may bias the model since it may learn this pattern and thus fail to generalize. If this pattern does exist in the dataset, corrective measures need to be taken such that the event hits in each timeslice are uniformly distributed.

To verify the existence of such patterns in the dataset, the mean time of event hits across all events was visualized as a scatter plot as depicted by Figure 4.3. A uniform

	pos_x	pos_y	pos_z	time	label	event_id	timeslice
pos_x	1.00	-0.01	-0.00	-0.00	0.00	-0.02	-0.00
pos_y	-0.01	1.00	0.00	0.00	-0.00	0.00	0.00
pos_z	-0.00	0.00	1.00	-0.00	0.00	-0.01	-0.00
time	-0.00	0.00	-0.00	1.00	-0.00	-0.01	1.00
label	0.00	-0.00	0.00	-0.00	1.00	nan	-0.00
event_id	-0.02	0.00	-0.01	-0.01	nan	1.00	-0.01
timeslice	-0.00	0.00	-0.00	1.00	-0.00	-0.01	1.00

Figure 4.2: Correlation matrix of features

Table 4.2: Descriptive statistics

	x	y	z	t	label	event_id	timeslice
count	4.58e+7	4.58e+7	4.58e+7	4.58e+7	4.58e+7	489906	4.58e+7
mean	1.16e-02	-1.59e-02	1.17e+02	5.00e+07	1.06e-02	2862.00	3.33e+03
std	5.12e+01	6.22e+01	4.86e+01	2.89e+07	1.02e-01	1667.61	1.92e+03
min	-9.46e+01	-1.15e+02	3.77e+01	0.00e+00	0.00e+00	0.00	0.00e+00
25%	-4.50e+01	-5.79e+01	7.40e+01	2.50e+07	0.00e+00	1392.25	1.66e+03
50%	1.30e+00	-4.18e+00	1.21e+02	5.00e+07	0.00e+00	2887.00	3.33000e+03
75%	4.04e+01	4.85e+01	1.60e+02	7.50e+07	0.00e+00	4304.75	5.00000e+03
max	9.62e+01	1.05e+02	1.96e+02	1.01e+08	1.00e+00	5734.00	6.77e+03

distribution is noted with no visible patterns. Thus no bias exists in the dataset and it is deemed suitable for further analysis.

4.3 Exploration of Interesting Timeslices

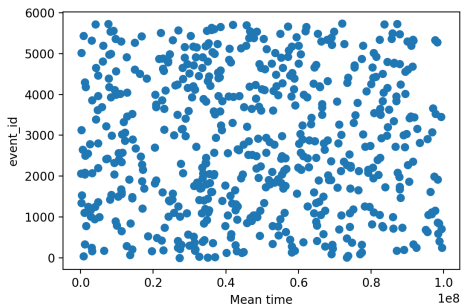

Figure 4.3: Verification of Bias

Figure 4.4 represents to total number of event hits per timeslice. The dataset is discretized into 6759 timeslices of which 2783 timeslices contain only noise hits. This is corroborated by Figure 4.4 which presents a skewed distribution where many timeslices contain few to no event

hits and few timeslices contain a high number of event hits.

Figure 4.5 depicts a scatter plot of *timeslice 615* which contains the largest number of event hits. It is observed that event hits occur close to each other in space and time (represented by the yellow, blue and green points) whilst background hits are uniformly distributed in space and time (represented by the purple points).

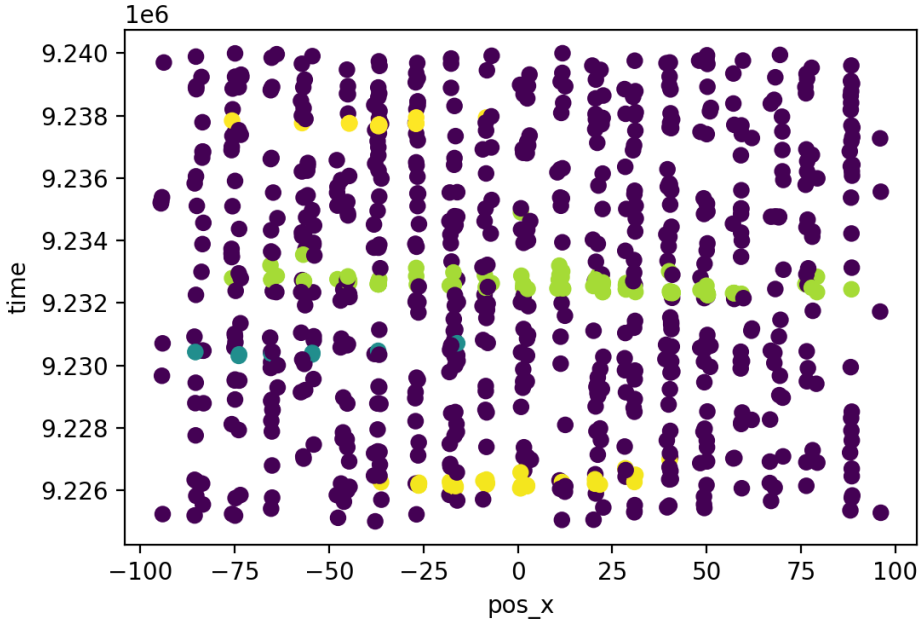

Figure 4.5: Distribution of Timeslice 615

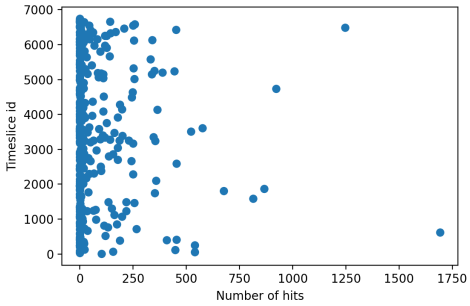

Figure 4.4: Distribution of event hits per timeslice

5

Replacement for Hit Correlation Step

This chapter presents the replacement created using a Multi Layered Perceptron (MLP) for the *Hit Correlation Step* of the Karas pipeline (see 2). It is observed that a MLP is able to identify causally related hits with a higher accuracy, precision and recall compared to the PMC. The chapter begins by explaining how the data is created followed by its visual examination. The training and testing procedure for the model is explained next. The chapter concludes with discussions of the experiment results and next steps.

5.1 Data Preparation

Figure 5.1 summarizes the MLP dataset creation process. With an input data of shape $(n, 4)$ (n rows and 4 columns representing *x, y, z, and t*), an output data of shape $(\sum_{k=n-1}^{1} k,\ 9)$ is obtained. A significant rise in the number of rows is observed since each row (representing a single hit) is paired with all rows that follow. The output dataset consists of 9 columns due to the presence of *x, y, z and t* columns of two hits plus the label column.

The label column is populated based on the values of the `event_id` column of the two hits. The row is assigned a label of 1 if the two hits have the same event id, which signifies that they originated from the same neutrino event and hence are causally related to each other. If the event id of the two hits are not the same then they are assigned a label of 0.

Better model performance was observed when the model was trained with the difference between hits in time and space. As a result, the final dataset of shape $\sum_{k=n-1}^{1} k,\ 5$ was obtained. The fist 4 columns being the difference of *x, y, z and t* vectors of the paired hits and the last column being the label. The data is additionally scaled between $[0, 1]$ as

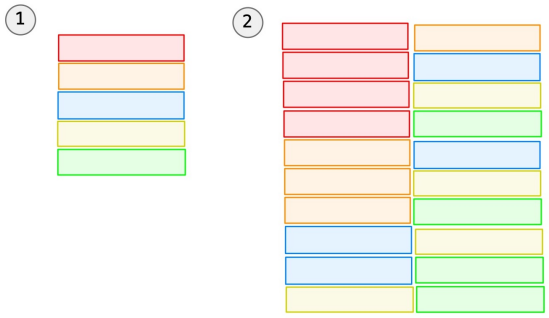

Figure 5.1: Overview of MLP dataset creation procedure. **(1)** The main dataset where each row represents a hit, here an example set containing 5 rows is shown for simplicity. **(2)** The MLP dataset is generated from the main dataset consisting of all unique pairs of hits. Algorithmically, this is done by pairing each hit with the subsequent hits below it as demonstrated with the use of colors. **(3)** The difference between the hits is taken (dark orange) and a label is assigned to each row (gray).

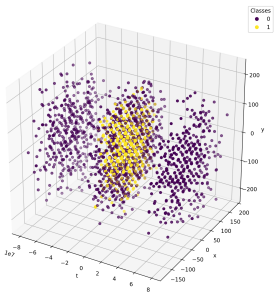

Figure 5.2: Distribution of MLP training dataset.

this is recommended and empirically proven to improve model performance and prevent vanishing gradients during training **??**.

5.1.1 Preparation of Training Data

The main dataset is highly skewed, with the **majority or negative class** being hits from background noise and the **minority or positive class** being hits from neutrino events. Thus, the training set created is also skewed with the minority class being related hits and majority class being unrelated hits. To maximize the number of positive examples in the training set, a random sample was taken from the top 5 timeslices of the main dataset with the most number of event hits. The model is required to classify related and unrelated hits which can be done by observing the space and time difference between the given points. Since this phenomenon is consistent across the entire main dataset, training using a sample does not introduce any bias into the model.

The training set still however contains a skewed distribution of examples, and training the model with such a dataset will result in a model that is biased to the majority class. To combat this problem, the majority class is *undersampled* such that the number of examples for each class is the same. Figure 5.2 shows the distribution of a random sample of the training set. It is observed that the related hits occur close to one another in space and time whilst the noise hits are scattered throughout which should aid the model to learn.

A fraction of the training set is kept as a hold out or validation set to evaluate the model's training. Table 5.1 presents the distribution of the training and validation sets.

Table 5.1: Distribution of MLP Training and Validation Datasets.

	Total examples	Positive examples	Negative examples
Training	48,434	24,217	24,217
Validation	23,856	11,928	11,928

5.1.2 Preparation of Testing Data

Whilst the training dataset contains equal number of examples for each class, the testing dataset maintains it's skewed distribution since this represents realistic data which the model will be required to classify. Four variants of the testing dataset with varying level of examples of related hits were created as listed in Table 5.2. In practice, the pipeline will observe timeslices which contain no to very few related hits, thus the performance of the model on TS1 and TS2 are of vital importance.

Table 5.2: Distribution of MLP Test Datasets.

	Total examples	Positive examples	Negative examples
TS1	774,390	–	774,390
TS2	5,829,405	10	5,829,395
TS3	5,880,735	1176	5,879,559
TS4	364,231	8,372	355,859

5.2 Model Description

The expectation of the model is to identify if two given points are causally related to each other or not. As revealed through data exploration in Chapter **??**, hits originating from neutrino events occur close to each other in space and time. Thus, The expectation from the model is to learn this phenomenon by training over pairs of points and classify unseen data as related or unrelated.

The parameters of the model are summarized in Table **??**. The Adam optimizer with a learning rate of 0.001 is used to optimize the loss function since it is considered a reasonable start for many optimization problems and has been empirically proven to outperform other algorithms such as *Stocastic Gradient Descent (SGD)*, *RMSProp* and *Adagrad* (8). Being

Loss	BCELoss
Optimizer	Adam
Learning rate	0.001
Hidden activation function	ReLU
Output activation function	Sigmoid
Training batch size	16
Testing batch size	32

Table 5.3: GCN Model Parameter Summary.

a binary classification task, the *Binary Cross Entropy Loss (BCELoss)* (also known as *Log Loss*) was selected as the loss function since it has been established as the standard loss function for binary classification tasks (9). As the BCELoss function expects an input in the range of $[0, 1]$, the *Sigmoid* activation function was chosen for the output layer. The *ReLU* activation function was chosen for the hidden layers since it is generally considered a good start for most problems (10, 11). A batch size of 16 is used for the training and validation sets whilst a larger batch size of 32 is used for the testing set since these value are often recommended as good defaults by machine learning practitioners (12, 13).

Layer Position	Type	Activation	Number of Neurons
1 (input)	Linear	–	4
2 (hidden)	Linear	ReLU	16
3 (hidden)	Linear	ReLU	8
4 (output)	Linear	Sigmoid	1

Table 5.4: MLP Model Architecture Summary.

The model architecture is summarized in Table 5.4. It consists of an input layer, two hidden layers and an output layer. The network is fully connected with 4 neurons in the input layer, 16 neurons in the first hidden layer, 8 in the second hidden layer and finally 1 neuron in the output layer. The optimal value of all parameters stated above were identified either empirically or from recommendations presented in literature. The number of epochs used to train the model is not mentioned above since this parameter is largely determined by the dataset, batch size and the learning rate, thus its value varied per experiment.

5.3 Model Evaluation

The model is evaluated using several metrics which are regarded as the standard set of metrics to evaluate machine learning model. Additionally, metrics geared towards evaluating a model performing binary classification on skewed datasets are considered as well.

1. **Accuracy**. The accuracy is the ability of a model to classify unseen data correctly and is mathematically defined by Equation 5.1.

$$Accuracy = \frac{Numberofcorrectpredictions}{Totalnumberofexamples} \tag{5.1}$$

2. **Learning Curve**. The Learning curve is a line plot of the loss over the training epochs. A model with a good fit results in a loss curve which approaches 0 with time.

3. **Confusion Matrix (CM)**. For highly skewed data, accuracy is not a good metric for evaluating the model performance (14) since it may achieve a high score by simply predicting the majority class. Thus the CM is used to visualize the number of *true positive (TP)*, *true negative (TN)*, *false positive (FP)* and *false negative (FN)* predictions of the model.

4. **Recall**. The recall is the ability of the model to correctly identify the minority class. For this problem, the recall of the model is given precedence over its precision. This is because the model should be able to identify all instances of the positive class since this determines if the timeslice will ultimately be saved or not. The recall is mathematically defined by Equation 5.2.

$$\frac{TP}{TP + FN} \tag{5.2}$$

5. **Precision**. The precision is the ability of the model to not misclassify an instance of the negative class (ie. classify it as the positive class). Although this should also be high, it is often inversely proportional to recall. The precision is mathematically defined by Equation 5.3.

$$\frac{TP}{TP + FP} \tag{5.3}$$

6. **F1 score**. The F1 score is the harmonic mean of the precision and recall, thus it is a single metric to summarize the model's performance based on its precision and recall. The F1 score is a value between $[0, 1]$ with a value close to 1 indicating high precision and recall. The F1 score is mathematically defined by Equation 5.4.

$$\frac{2 * (Precision * Recall)}{Precision + Recall} \tag{5.4}$$

7. **F2 score**. Since recall is given precedence for this problem, the F2 score can be considered a better alternative to the F1 score as it gives higher importance to the recall through the β parameter. The F2 score is mathematically defined by Equation 5.5. Thus the F2 score with $\beta = 1$ is equivalent to the F1 score.

$$\frac{(1 + \beta^2) * Precision * Recall}{(\beta^2) * (Precision + Recall)} \tag{5.5}$$

8. **Receiver Operating Characteristic (ROC) curve** is a plot of the *true positive rate (TPR)* and the *false positive rate (FPR)* (mathematically defined by Equations 5.6) across various discrimination probability thresholds of the model. The ROC curve can be interpreted as the fraction of correct predictions for the positive class (along the y-axis) versus the fraction of error in predictions for the negative class (along the x-axis). The area under the ROC curve (ROCAUC) can be used to summarize the ROC curve with a singular value. Thus, a highly skilled model has a ROC curve which arches from $(0, 0)$ to $(1, 1)$ with a ROCAUC between 0.5 and 1.0. Whilst the ROC curve of a model without any skill is a straight line from $(0, 0)$ to $(1, 1)$ with a ROCAUC of 0.5.

$$TPR = \frac{TP}{TP + FN} FPR = \frac{FP}{FP + TN} \tag{5.6}$$

9. **Precision-Recall (PR) Curve** can be considered a better alternative to the ROC curve since the ROC curve can be overly optimistic of the model's skill when dealing with highly skewed data since it considers the model's performance for both the classes. In contrast, the PR curve is a diagnostic plot of the model's precision and recall across various discrimination probability thresholds of the model. Thus the PR curve only considers the model's performance with regards to the positive class. Similar to the ROC curve, the PR curve can also be summarized by the area under the curve or the PRAUC. A skilled model, thus has a PR curve which bows towards $(1, 1)$ whilst a model with no skill is a horizontal line.

5.4 Results

Figure 5.4 shows the learning curve of the model on the training and validation tests. The curves approach zero with time and remain in close proximity to each other indicating a good fit. Table 5.4 summarizes the model's performance across the various test sets (see Section 5.1.2). In general, the model performs well with high accuracy and recall across all test sets. The model achieves almost perfect recall for TS2 and TS3 which have extremely low positive examples which speaks to its strength. The poor precision scores can be attributed to the skewed nature of the datasets. Since the FPs are relatively high compared to the TPs in the datasets, the precision falls drastically. This is also corroborated by the fact that the recall in TS4 increases due to a better FP:TP ratio (see Figure 5.19).

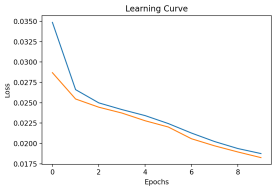

Learning Curve of MLP Training and Validation Datasets.

	Accuracy	Precision	Recall	F1	F2	ROCAUC	PRAUC
TS1	0.80	–	–	–	–	–	–
TS2	0.91	0.00	1.00	0.00	0.00	0.99	0.00
TS3	0.92	0.00	0.98	0.00	0.01	0.98	0.01
TS4	0.92	0.19	0.83	0.31	0.48	0.96	0.33

Summary of MLP performance across test sets.

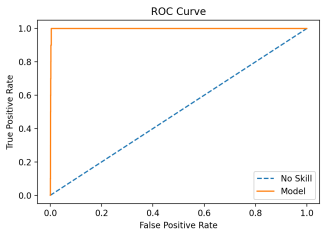

Figure 5.3: ROC Curve for TS2.

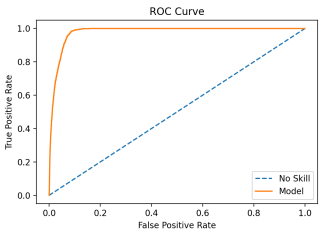

Figure 5.4: ROC Curve for TS3.

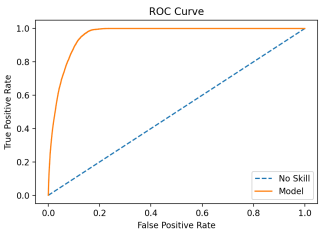

Figure 5.5: ROC Curve for TS4.

Figure 5.6: ROC Curves for MLP Test Datasets.

The ROC curves paint a different picture (see Figure 5.6) with exceedingly high areas. This however is misleading since ROC curve takes into account the performance for both the positive and negative classes and thus tend to be overly optimistic of the model's performance on skewed datasets (14, 15). In such circumstances, The PR curves are considered better at gauging a model's skill when dealing with skewed datasets (14). However, in this case it too is deemed misleading as it seriously undermines the model's performance (see Figure 5.10). This again is attributed to the precision approaching zero due to the

extremely skewed FP:TP ratio which results in the PRAUC to also be zero.

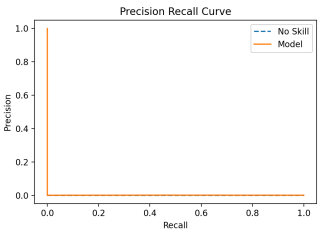

Figure 5.7: PR Curve for TS2.

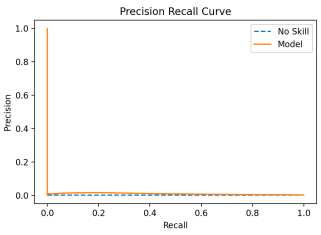

Figure 5.8: PR Curve for TS3.

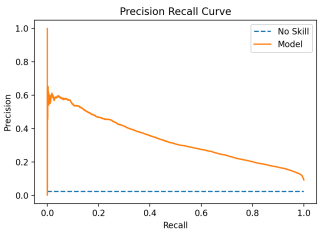

Figure 5.9: PR Curve for TS4.

Figure 5.10: PR Curves for MLP Test Datasets.

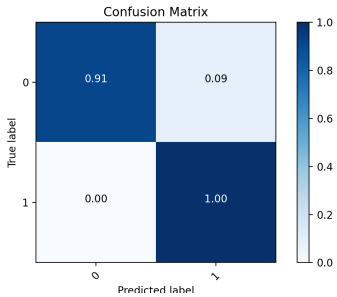

Figure 5.11: Norm Confusion Matrix for TS2.

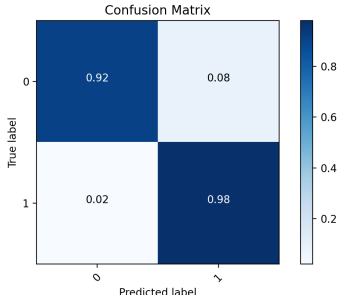

Figure 5.12: Norm Confusion Matrix for TS3.

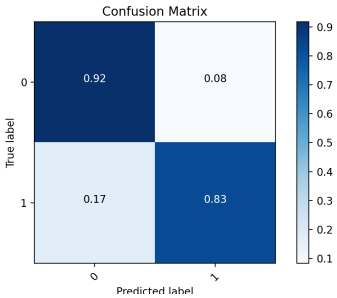

Figure 5.13: Norm Confusion Matrix for TS4.

Figure 5.14: Normalized Confusion Matrices of MLP Test Datasets.

Figure 5.19 depict the confusion matrices for the various test datasets. Alternatively, Figure 5.14 can also be consulted which presents the confusion matrices normalized across the rows. The confusion matrices highlight the strengths and weaknesses of the model better than the ROC and PR curves. The model has a very low number of FNs and FPs which is extremely valuable as this ensures that the model does not miss hits from neutrino events and also does not classify hits from noise sources incorrectly as hits from neutrino events.

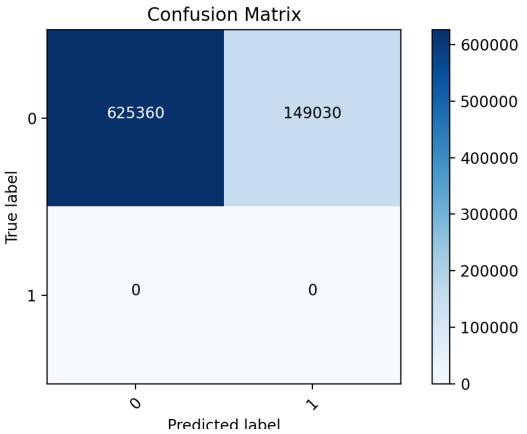

Figure 5.15: Confusion Matrix for TS1.

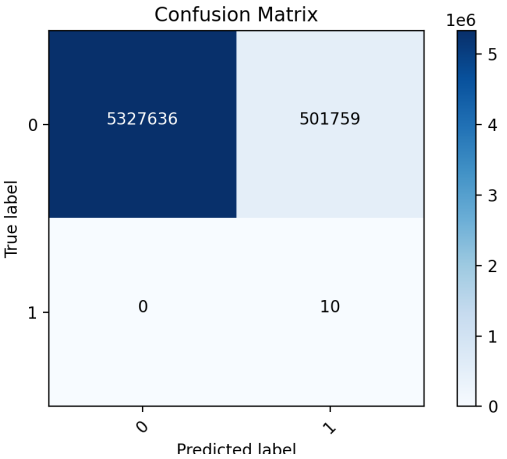

Figure 5.16: Confusion Matrix for TS2.

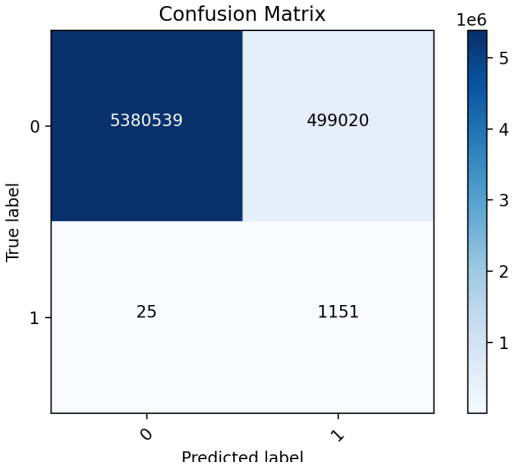

Figure 5.17: Confusion Matrix for TS3.

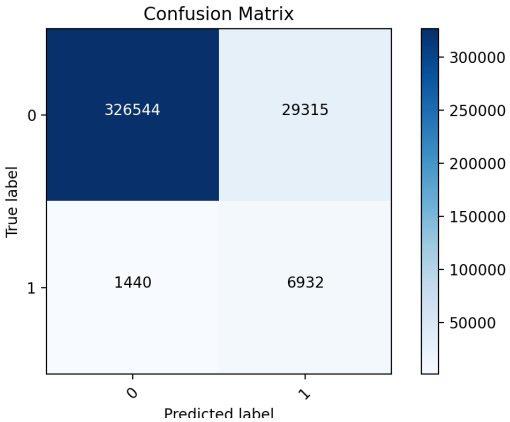

Figure 5.18: Confusion Matrix for TS4.

Figure 5.19: Confusion Matrices of MLP Test Datasets.

6

Replacement for Graph Community Detection Step

This chapter presents the replacement created using a Graph Convolusional Neural Network (GCN) for the *Graph Community Detection Step* of the Karas pipeline (see **??**). It is observed that a GCN is able to classify noise and event nodes very well, even in extremely skewed datasets with less than 10 event nodes. The chapter begins with an overview of GCNs and how they have been applied to this problem. The data preparation, visualization and model evaluation are touched upon next. The chapter concludes with discussion of the results and next steps.

6.1 Primer on Graph Convolusional Neural Networks

6.1.1 GNN and graphs

GNNs are designed to operate on data which can be represented as graphs. A graph consists of nodes and edges. Each node may or may not be connected to one or many nodes, these are referred to as the neighbors of the node. A graph with all nodes connected to one another is called a fully connected graph.

An edge may have attributes associated with it, the two most common attributes being weight and direction. An edge may be directed which denotes a sense of hierarchy amongst the nodes, or undirected. An edge may also have a weight to signify a stronger or weaker connection amongst nodes.

Nodes may also posses attributes associated with themselves, commonly known as node embeddings. The complexity of the node embedding may range from a simple scalar quan-

tity to a multi-dimensional tensor, and depends on the dataset and how the practitioner wishes to sculpt the graph.

Graphs are primarily classified into two variants.

1. **Homogeneous graphs**. Graphs with the same type of nodes and edges are referred to as homogeneous graphs. For example, a graph representing who follows who on Twitter is a homogeneous graph. Here, people are represented as nodes and an edge indicates that person A follows person B.

2. **Heterogeneous graphs**. Graphs with different types of nodes and edges are referred to as heterogeneous graphs. For example, a graph representing a person's likes and dislikes in regards to food items. Here, two entities, namely people and food are represented as nodes. The edges also come in two variants ie. a 'like' and a 'dislike'.

6.1.2 The Message Passing Paradigm

During each training epoch, a node propagates it's embedding to it's neighbors and in return receives their embedding. All collected embeddings are aggregated (for example using a sum, difference or mean) which becomes the new embedding of the node. This procedure is done for all nodes of the graph, for each training epoch. The number of layers in the network determine how far the messages are sent. For example, for a network with a single layer, each node sends a message to it's immediate neighbors. With 2 layers, the node also sends a message to the neighbors of it's immediate neighbors and so forth.

6.2 Data Preparation

The graphs for the testing and training of the network are constructed from a combination of the main dataset and a modified version of the MLP dataset, Figure 6.1 illustrates this procedure. A fully connected graph is constructed, and its node embeddings and node labels are derived from the main dataset. Thus, each node is thus assigned a (x, y, z, t) vector as it's node embedding. The node is assigned a label of 1 if it is an event hit, else a label of 0.

A modified MLP dataset (see 5.1) with a shape of $(n^2 - n, 5)$ is created such that each hit is paired with all other hits except itself. The label column from this dataset is then used as the edge weights of the graph. Edges between event nodes from the same event thus are assigned a weight of 1 and all other edges are assigned a weight of 0.

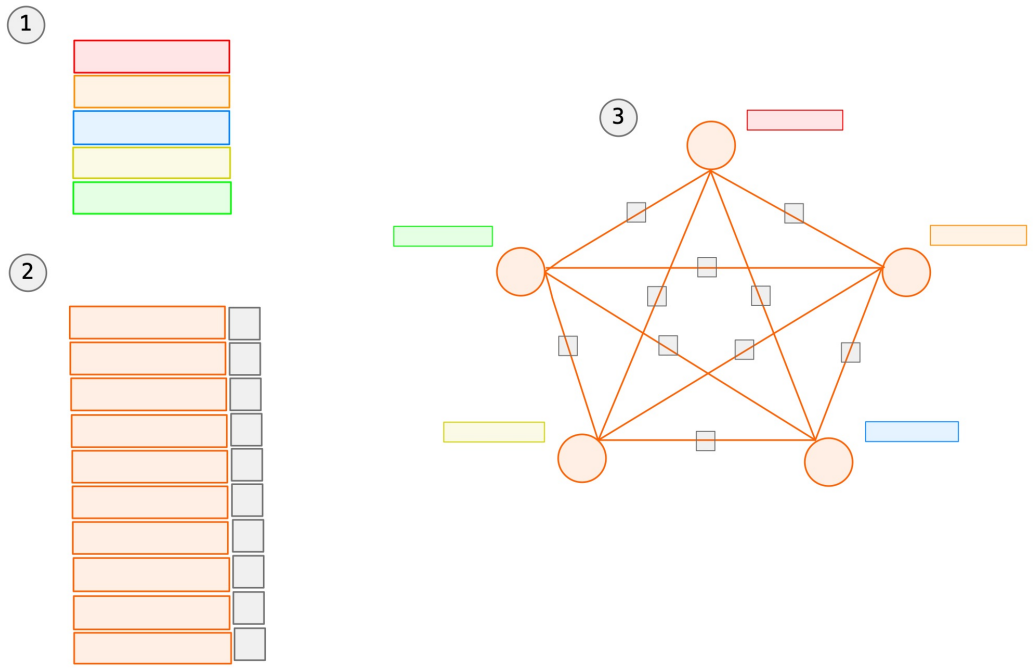

Figure 6.1: Overview of GCN dataset creation procedure. **(1)** an example of the main dataset with 5 hits. **(2)** the corresponding modified MLP dataset created. Although the dataset will contain $n^2 - n = 25$ rows, only the unique rows (10 in this example) are shown in the illustration for simplicity. **(3)** The graph representation is created where rows of (1) become the node embeddings and the label column of (2) become the edge weights.

Since the main dataset and the pattern matrix dataset are highly skewed, naturally the GCN dataset is also skewed with majority of the nodes being noise. Similar strategy as used in the creation of the pattern matrix training set (see 5.1) is used. The training set is a graph with 1000 nodes equally distributed amongst the classes.

The skewed nature of the data is maintained in the testing set. The model is evaluated with 3 test sets each with varying levels of examples of event nodes. In practise, the pipeline will observe timeslices with no to very few events thus the performance of the model on test set 1 and 2 should be given importance.

TS1. No event nodes

TS2. Less than 25 event nodes

TS3. Less than 250 event nodes

Loss	BCELoss
Optimizer	Adam with learning rate of 0.001
Hidden Activation	ReLu
Output Activation	Sigmoid

Table 6.1: GCN Model Parameter Summary.

6.3 Model Description and Evaluation

The model is expected to classify nodes of an unseen graph as event or noise nodes. Since causally related nodes are connected with edges carrying a high weight, the model is expected to group them together thus resulting in a final graph with small clusters of causally related nodes and a large clusters of noise nodes.

The parameters of the model are summarized in Table 6.1, the rational for selecting the parameters being the same as that of the pattern matrix model (see 5.2) since both models perform binary classification. The difference comes from the model architecture. The GCN model comprises of an input layer, two graph convolusional layers and an output layer. The network is fully connected with 4 neurons in the input layer, 16 in both graph convolusional layers and 1 neuron in the output layer.

Evaluation metrics used for evaluating the MLP model are used to evaluate the GCD model as well (see Section 5.3) since the GCN dataset is also highly skewed in nature.

6.4 Discussion

7

Recommendations

This chapter presents some practical recommendations for the readers who wish to use the new data processing pipeline presented in this report. The chapter also presents alternative paths of research which remain unexplored and general improvements that can be made to the pipeline in the future.

Chapter **??** presented a Multi Layered Perceptron capable of identifying causally related hits with a higher accuracy, precision and recall compared to the Pattern Matrix Criterion presented by Karas et al. The PM model is seem as a viable successor to the PM Criterion. The model can be further improved using larger training sets and the model performance can be improved by utilizing the plethora of techniques.

The output of the MLP is observed to be primitive (see Section **??**). As proved empirically, the GCD model is able to perform better when the edge weights are assigned based on the type of connection between the nodes (see Section **??**). In order to obtain the advanced edge weight scheme, the MLP must be modified such that it performs multi-class classification on the edge types. For a classification problem of n edge types, the output of the MLP will thus become a `(n,)` vector containing the expected probability for each class. These probabilities can then be used as the edge weights.

Chapter **??** presented a Graph Convolusional Neural Network capable of identifying event nodes with immaculate accuracy, precision and recall in extremely skewed datasets. The network however have a very high false positive rate when tested with a set containing no event nodes. This bias may be removed by framing the data as a multi-edge, heterogeneous graph. The model is thrown off by the high weights on edges between causally related event nodes and noise nodes. Thus by creating different types of edges corresponding to the various types of connections that two nodes may posses (see **??**), each carrying the corresponding weights, the network may be able to correct it's bias to the positive class.

7. RECOMMENDATIONS

The models presented in this report were testing in isolation. However the intended use is to combine them in order to identify timeslices containing neutrino event hits (see Section **??**). Thus the models should be tested as an integrated pipeline in order to determine if feasible as improvement over the Karas pipeline.

Results from the GCD experiments (see Section **??**) indicate that the model is unable to learn anything from the node embeddings thus identifying better node embeddings to help the enhance the model's learning abilities remains open to be examined. The network currently aggregates the node embeddings by adding them. This however may not be an apt aggregation function and the model's performance needs to be compared with alternatives such as the difference and mean.

An alternative path of research exists to explore the possibility of replacing the entire pipeline with a single GNN. The data can be framed such that the `(x, y, z)` vector is used as the node embedding and δt between the nodes is used as the edge feature.

Finally, the problem can also be framed as a graph classification problem. The expectation being that the network is able to identify clusters of causally related nodes from noise.

Bibliography

[1] Annarita Margiotta, KM3NeT Collaboration, et al. **The KM3NeT deep-sea neutrino telescope**. *Nuclear Instruments and Methods in Physics Research Section A: Accelerators, Spectrometers, Detectors and Associated Equipment*, **766**:83–87, 2014. 1

[2] Silvia Adrian-Martinez, M Ageron, F Aharonian, S Aiello, A Albert, F Ameli, E Anassontzis, M Andre, G Androulakis, M Anghinolfi, et al. **Letter of intent for KM3NeT 2.0**. *Journal of Physics G: Nuclear and Particle Physics*, **43**(8):084001, 2016. 1, 2

[3] Sebastiano Aiello, Fabrizio Ameli, Annarita Margiotta, Michel Andre, Giorgos Androulakis, Marco Anghinolfi, Antonio Marinelli, Gisela Anton, Miquel Ardid, Christos Markou, et al. **KM3NeT front-end and readout electronics system: hardware, firmware, and software**. *Journal of Astronomical Telescopes, Instruments, and Systems*, **5**(4):046001, 2019. 2

[4] Maarten Post. *"KM3NNeT" A neural network for triggering and classifying raw KM3NeT data*. PhD thesis, Universiteit van Amsterdam, 2019. 2, 3

[5] Konrad Karaś. *Data processing pipeline for the KM3NeT neutrino telescope*. PhD thesis, Universiteit van Amsterdam, 2019. 2, 5

[6] **NumPy - The fundamental package for scientific computing with Python**. 9

[7] **Pandas**. 10

[8] Sebastian Ruder. **An overview of gradient descent optimization algorithms**. *arXiv preprint arXiv:1609.04747*, 2016. 17

[9] Amichai Painsky and Gregory Wornell. **On the universality of the logistic loss function**. In *2018 IEEE International Symposium on Information Theory (ISIT)*, pages 936–940. IEEE, 2018. 18

[10] Chigozie Nwankpa, Winifred Ijomah, Anthony Gachagan, and Stephen Marshall. **Activation functions: Comparison of trends in practice and research for deep learning**. *arXiv preprint arXiv:1811.03378*, 2018. 18

[11] Gang Wang, Georgios B Giannakis, and Jie Chen. **Learning ReLU networks on linearly separable data: Algorithm, optimality, and generalization**. *IEEE Transactions on Signal Processing*, **67**(9):2357–2370, 2019. 18

[12] Yoshua Bengio. **Practical recommendations for gradient-based training of deep architectures**. In *Neural networks: Tricks of the trade*, pages 437–478. Springer, 2012. 18

[13] Ian Goodfellow, Yoshua Bengio, and Aaron Courville. *Deep Learning*. MIT Press, 2016. `http://www.deeplearningbook.org`. 18

[14] Paula Branco, Luis Torgo, and Rita Ribeiro. **A survey of predictive modelling under imbalanced distributions**. *arXiv preprint arXiv:1505.01658*, 2015. 19, 21

[15] Alberto Fernández, Salvador García, Mikel Galar, Ronaldo C Prati, Bartosz Krawczyk, and Francisco Herrera. *Learning from imbalanced data sets*. Springer, 2018. 21